Nickel impurities in the Y-Ba-Cu-O 90-K superconductor

M. Qian, E. A. Stern, Y. Ma, and R. Ingalls
Department of Physics, FM-15, University of Washington, Seattle, Washington 98195

M. Sarikaya, B. Thiel, R. Kurosky, C. Han, L. Hutter, and I. Aksay
Department of Materials Science and Engineering, FB-10, and Advanced Materials Technology Program, Washington Technology Center, University of Washington, Seattle, Washington 98195

(Received 15 June 1988; revised manuscript received 24 August 1988)

The orthorhombic superconductor $YBa_2(Cu_{1-x}Ni_x)_3O_{7-\delta}$ with nominal values of $x=0.02$ and 0.05 and $T_c=86.5$ and 79.5 K, respectively, was investigated by x-ray-absorption fine-structure (XAFS) measurements about the Ni and Cu K edges. The sample was carefully characterized by various means including optical and electron microscopy. In the sample with $x=0.02$, the Ni was predominantly dissolved in the 1:2:3 phase. The maximum solubility found in the nominal 5% phase was $x=0.04$, with the excess precipitating out as NiO. The Ni atoms in the 1:2:3 phase were found to have 4.75 ± 0.4 oxygen neighbors at 1.95 ± 0.03 Å. The best fit to the next neighbor was 5.1 ± 1.2 Y atoms at 2.96 ± 0.02 Å, though the data are also consistent with a mixed shell of Y and Ba atoms. Although the Ni atoms have a first-neighbor environment of oxygen atoms somewhat similar to the Cu site, the more distant neighbor distances are quite different. It is concluded from both the extended and near-edge XAFS that most, if not all, of the Ni atoms do not substitute in either Cu site of the 1:2:3 phase, but are in some defect site.

INTRODUCTION

The basic pairing mechanism of high-T_c superconductors is still not experimentally clarified. All of the present materials that exhibit high-T_c above liquid-nitrogen temperatures have in common copper oxides as a component in a perovskitelike structure. When Cu atoms are substituted by other atoms the value of T_c usually decreases. To investigate this phenomenon with the goal of obtaining more insight into the unique role of Cu, we have investigated $YBa_2(Cu_{1-x}Ni_x)_3O_{7-\delta}$ with Ni nominally substituted for Cu. It has been found[1] that such a substitution decreases T_c and comparing the environment about the Ni to that about the Cu atoms may give a clue as to what properties of the Cu atoms are crucial to high T_c.

There have been many experiments performed on substituting for the various metal atoms in the 1:2:3 high-T_c superconductor.[1–18] They can be summarized by the observation that the substitution for Cu has the largest impact on the superconducting properties. However, most of the experiments on Cu substitution have not been able to verify where the impurity atom actually resides in the sample. Only recently have there been attempts to obtain such detailed information using neutron diffraction,[13,15] x-ray-absorption fine-structure (XAFS) measurements,[17,18] and Mössbauer spectroscopy.[16] We present here a detailed investigation combining the XAFS technique with a careful characterization of the morphology of the sample.

SAMPLE PREPARATION AND CHARACTERIZATION

All samples were made using Y_2O_3, BaO_2, and CuO powders. To meet stoichiometry requirements, the Cu mole ratio was reduced and replaced by the Ni mole ratio to form $YBa_2(Cu_{1-x}Ni_x)_3O_{7-\delta}$. The doping agents used were NiO powder and $Ni(OAc)_24H_2O$ (nickel acetate) at three different molar ratios corresponding to $x=0.02$, 0.05, and 0.09. In order to enhance the mixing of the metal oxides with the doping powders, the initial raw materials for each sample were dispersed in either ethyl alcohol or acetone with the aid of ultrasonication and dried in a rotary evaporator to prevent possible long-range phase separation during solvent removal. The dried mixing powders were then uniaxially die pressed at $>20\times10^3$ psi into $\frac{3}{4}$ in. diameter disks and sintered following the standard heat-treatment schedule given below.

Optical micrographs of the NiO doped samples showed large grains (~40 μm in diameter) of NiO in each of the samples, independent of x. Only the number changed with x. The x-ray-diffraction patterns also showed a multiphased sample. Because of this obvious multiphase morphology, these samples were not suitable for our purposes and samples using Ni acetate as the doping agent were prepared. Ni acetate was chosen because of its low melting temperature of 16 °C and its partial solubility in alcohol. Samples were heated at 5 °C/min to 950 °C and held for 2 h in slightly flowing air. Samples were cooled at 1 °C/min to room temperature and ground with mortar and pestle to a fine powder and repressed at $>45\times10^3$ psi. These samples were once again heat treated to 950 °C but held for only 1 h and again cooled at 1 °C/min to room temperature. Although the 2% and 5% samples gave a single-phase x-ray powder-diffraction pattern, another regrind and sintering step was performed. The final heat treatment of the samples also was done at 950 °C for 1 h and cooled to room temperature at 1 °C/min.

The samples were characterized by x-ray diffraction, ac

 ©1989 The American Physical Society

magnetic-susceptibility (20 Hz, ~2 G rms), electrical resistance, and optical and electron microscopy. For $x=0.02$ and 0.05 the samples were found to be superconducting, exhibiting zero resistance and magnetic shielding with $T_c=86.5$ and 79.5 K, respectively, as defined by the midpoint of the ac magnetic-susceptibility curve. The susceptibility indicated that over 90% of the volume of the samples expelled the flux. The x-ray diffraction did not detect any impurity phases, only the orthorhombic superconducting phase, with $a=3.817$ and 3.818, $b=3.886$ and 3.878, $c=11.674$ and 11.655 for the values of $x=0.02$ and 0.05, respectively. The dimensions are in Å and the uncertainties are about 0.002 Å. In contrast when $x=0.09$, the x-ray diffraction indicated a multiphase sample, and no superconducting transition was found.

According to a standard common in the literature, the x-ray-diffraction results would be interpreted to indicate that the 2% and 5% samples were a single phase of $YBa_2(Cu_{1-x}Ni_x)_3O_{7-\delta}$. However, the sensitivity of powder x-ray diffraction is limited and we therefore characterized the samples more thoroughly and with much more sensitivity. The two main methods employed for this characterization were optical and transmission electron microscopy (TEM). In optical microscopy the surface of the sample was polished and then several different sections were photographed under a magnification of 400. Different phases were identified in the image by comparing with corresponding images in electron microscopy. In the TEM work the composition of the various phases was identified by energy dispersive x-ray spectroscopy (EDS) using a 40-nm electron probe and the quantification was done by standardless analysis.[19] Selected area diffraction confirmed the analysis with the diffraction patterns showing the unit-cell dimensions and symmetries of the crystal phases. In this manner the 1:2:3 and 2:1:1 YBaCuO phases and Cu_2O were identified.[20] All electron microscopy was performed on a Philips 430T operated at 300-keV accelerating voltage.

NiO was identified in the optical microscope by its greater hardness compared to the other phases. This revealed itself in the polishing of the samples. The NiO precipitates protruded from the surface and were recognizable by their shadowing around the boundary. A uniform grid was superimposed on the optical microscope photograph and the number of times the intersection points of the grid were located in various phases was recorded. In all, one thousand grid points were used. The results are summarized in Table I. The volume fraction of each phase is directly equal to the fraction of the total number of points recorded for each phase.[21]

Table I indicates that though the samples were mainly 1:2:3 phase, there were detectable amounts of 2:1:1 and other phases. Correcting for the voids the volume percentages of various phases in the two samples are presented in the fourth and fifth columns of Table I.

In the TEM the section of the sample that is viewed is much smaller than in the optical microscope. For that reason the assessment of the relative percentages of each phase by the TEM is not as statistically significant. However, the transmission TEM permits a more detailed analysis of each phase. Only the 5% Ni sample was investigated in the TEM. In the region of the sample viewed in the TEM, both 1:2:3 and 2:1:1 phases were visible. No grain boundary regions were visible, nor were Cu_2O or NiO phases seen. The 1:2:3 phase had Ni content relative to Cu varying from 3.3 to 4.0 ± 0.5 at.% while the 2:1:1 phase had 2.7 ± 0.5 at.%. Although only 1% of the 5% sample is composed of NiO, that phase still contains a significant amount of the total Ni and this must be accounted for in the analysis. Since no Ni-rich precipitate was seen for the 2% sample, and assuming that the relative Ni concentrations in the 1:2:3 and 2:1:1 phases are the same as for the 5% sample, then 94% of Ni is in the 1:2:3 phase for that sample.

To summarize the results of the sample composition by our characterization, the 2% sample has 94% of the Ni dissolved in the 1:2:3 phase with $x=0.02$. The 5% sample has the Ni signicantly mixed between the 1:2:3 phase with $x=0.04$ and the NiO precipitates.

XAFS MEASUREMENTS AND ANALYSIS

The XAFS measurements on the superconducting samples were made at room temperature on the Ni and Cu K edges at the Stanford Synchrotron Radiation Laboratory (SSRL) on beamline 4-1 using a double (220) Si crystal monochromator. The Cu K-edge measurements were made in transmission while the Ni K-edge measurements were made in fluorescence. Detuning the double-crystal monochromator to minimize the harmonic content of the transmitted x-ray beam did not decrease the second harmonic sufficiently. A signal from the second harmonic exciting Y fluorescence was detectable and contaminated the fluorescence signal from the Ni. It was necessary to insert a piece of float glass before the I_0 ionization

TABLE I. Volume fractions of various phases in Ni-substituted samples. (The errors in the Table are standard deviations.)

Phase	2 at.% Ni	5 at.% Ni	2 at.% Ni (corrected)	5 at.% Ni (corrected)	at.% Ni in the 5% Ni sample
1:2:3	0.837(12)	0.810(12)	0.880(13)	0.831(13)	3.7 ± 0.5%
2:1:1	0.106(10)	0.154(11)	0.111(11)	0.158(12)	2.7 ± 0.5%
Cu_2O	0.008(3)	0.001(2)	0.008(3)	0.001(2)	...
NiO	0	0.010(3)	0	0.010(3)	...
voids	0.049(7)	0.025(5)	...		

chamber to act as a total reflecting mirror. The glacing angle of the mirror was adjusted so that the fundamental was totally reflected while the second harmonic was not. This extra filtering eliminated the contamination of the Ni signal by the Y fluorescence. The incident x-ray intensity was monitored by the I_0 ionization chamber which absorbed about 25% of the intensity, and the fluorescence signal was detected by an ionization chamber, Soller slit assembly[22] with a Co filter. The Co filter was only moderately effective in selectively eliminating the x-ray background, presumably because a significant fraction was caused by L-edge fluorescence from the Ba atoms in addition to the quasielastic scattering of the incident beam. A one millimeter slit in the vertical dimension was placed before the float glass mirror to define the incident x-ray beam. A number of scans were taken of the Ni edge at each concentration so as to accumulate statistics of over 10^7 effective photons per energy point, limiting the shot noise in the data to one part in $(10^7)^{1/2}$. The actual number of photons detected is larger than the effective number of photons by the ratio $(1+A)$ where $A=4.4$ is the background divided by the K-edge signal.

The 5% Ni sample is known to have a significant amount of the Ni in the NiO phase while the 2% Ni sample has essentially all of its Ni in the 1:2:3 phase. Because the amount of NiO phase is small, its quantity is not well determined and we found the best manner to estimate how much Ni is in the NiO phase for the 5% sample was to subtract a variable weight of the NiO spectrum from the 5% spectrum and to determine the weighting factor by requiring that the resultant spectrum be the same as that of the 2% sample. We succeeded in this goal with the assumption that about 30% of the Ni was in the NiO phase. In the subsequent discussion, we will focus on the 2% sample which our characterization showed has its Ni essentially only in the 1:2:3 phase.

The data were analyzed by standard methods.[23] The pre-edge background was first subtracted and a cubic spline with one or two nodes was used to subtract the atomic background above the edge. The intersection of the spline with the edge step was used to normalize the data of the 2% sample and the resulting $\chi(k)$ weighted by k^3 is displayed in Fig. 1 by the solid curve. The zero of energy for calculating k was set at the middle of the edge step. For comparison, the corresponding $k^3\chi(k)$ for the Cu K edge is shown in Fig. 1 by the dashed curve. The magnitude of the transforms for the $k^3\chi(k)$ data of Fig. 1 are displayed in Fig. 2. The k range for all transforms are $1.9 \leq k \leq 11.4$ Å^{-1}, and Hanning functions of width at 4.0 Å^{-1} at the upper k limit and 1.0 A^{-1} at the lower k limit are used to smooth the transition of the data to zero. The error bars indicate the variation determined by analyzing independent scans. The data about the Cu edge have much smaller errors, as expected.

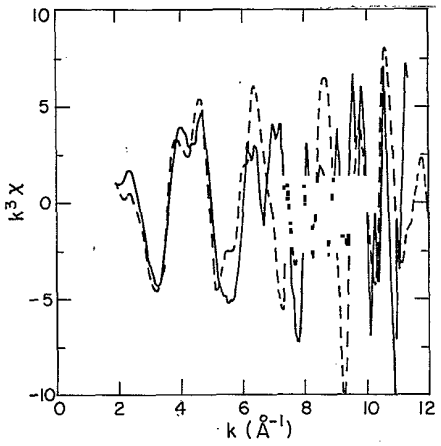

FIG. 1. Plots of $k^2\chi(k)$ for the Ni K edge (solid line) and for the Cu K edge (dashed line) of $YBa_2(Cu_{0.98}Ni_{0.02})_3O_{7-\delta}$.

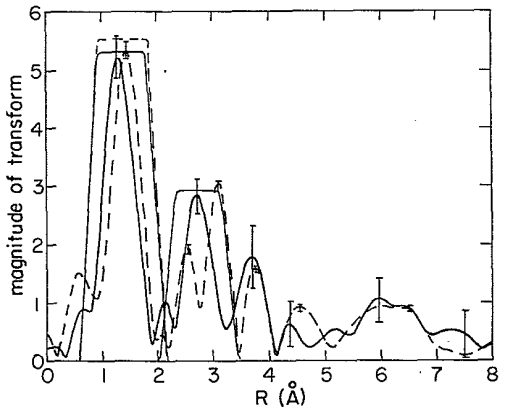

FIG. 2. The magnitude of the transform of the $k^3\chi(k)$ of Fig. 1. The Ni edge (solid line) and the Cu edge (dashed line) are transformed over the range $1.9 \leq k \leq 11.4$ Å with Hanning functions of width 1.0 and 4.0 Å^{-1} at the low and high ends of the range, respectively. The windows used for isolating particular shells are shown. The errors about the Cu edge are smaller.

RESULTS AND DISCUSSION

Figures 1 and 2 indicate that Ni is not simply substituting in the Cu site. The second and more distant peaks appear to be significantly different around the Ni and Cu atoms. To make a more quantitative comparison the ln ratio of amplitudes and differences in phase[23] were taken between various shells which were isolated using the windows shown in Fig. 2 and back transformed to K space. Since Cu and Ni are next to one another in the periodic table, differences in their center phase shifts are small and in our case we neglect this small difference in comparing their environments.

The ln ratio and phase differences of the first shell were taken between the 2% Ni sample and two models NiO and Ni acetate. The NiO data were taken at 300 K and the Ni acetate at 15 K, both in transmission. The NiO model did not give a very linear ln ratio versus k^2 plot but did give a reasonably linear phase difference. The ln ratio versus k^2 plot for Ni acetate is more linear and its phase difference plot is also reasonably linear at low k. These phase differences both gave reasonably consistent Ni-O distances of 1.95 ± 0.03 Å. The linear phase difference in Fig. 3(b) between Ni and Cu site in the 1:2:3 phase determined from the slope near $k=0$ indicates that the difference in average distance to the nearest neighbors is

$+0.01 \pm 0.03$ Å. This gives a consistent result of 1.94 ± 0.03 Å only if the large single Cu–O bond[24] at 2.3 Å is neglected (Table II). However, such neglect is expected because at room temperature, where our comparisons are made, the mean-square vibrational amplitude of this long bond is much greater than the shorter bonds and will give an insignificant contribution to the ln ratio and phase difference. Thus we should consider the Cu in the 1:2:3 phase as having four oxygen atoms at an average distance of 1.93 Å. The ln-ratio intercept is most reliable using the Ni acetate model and the Cu site as the model since they have the most linear plots, particularly at low k. The intercepts in Fig. 3(a) for these two cases give values of 5.0 ± 0.5 and 4.5 ± 0.5 O neighbors, respectively. Averaging these two values we obtain that there are 4.75 ± 0.4 oxygen neighbors around the Ni atoms at a distance of 1.95 ± 0.3 Å. The slope with the Ni acetate model indicates a value of $\Delta\sigma^2 = 0.003 \pm 0.003$ Å^2. Adding the structural disorder of Ni acetate to $\Delta\sigma^2$, the mean square disorder of the oxygen neighbors about their average value (including both structural and 300-K thermal) becomes $\sigma^2 = 0.004 \pm 0.003$ Å. The first neighbor environments about the Ni and Cu atoms are not too dissimilar and it has been stated,[17] on that basis alone, that the Ni substitutes for the Cu site.

A comment on Fig. 2 is appropriate at this point. Whereas the first peak around the Ni is ~0.1 Å shorter than that around the Cu, the phase differences in Fig. 3(b) was interpreted to indicate that the average first-neighbor distances around the Cu and Ni atoms are essentially the same. This apparent discrepancy occurs because the phase difference is not linear. The Fourier transform of Fig. 2 is sensitive to the average slope of the phase difference which, as seen in Fig. 3(b), is negative giving the shorter distance about the Ni. However, the true distance difference is obtained from the linear slope nearest the origin[23] which is approximately zero indicating little difference. Theory indicates[23] that differences in the odd moments of the radial distribution function of the first neighbors about the Ni and Cu atoms add variations in their phase difference to produce the nonlinear behavior,

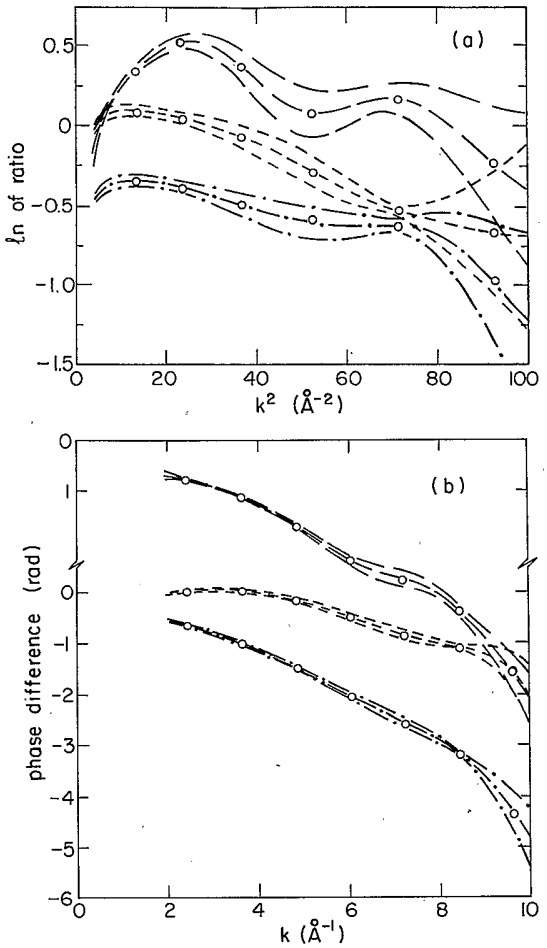

FIG. 3. (a) The ln ratio vs k^2 of the Ni K-edge XAFS of the 2% sample divided by the Ni-edge data of NiO (long dash line), Ni acetate (dash-dot line), and the Cu-edge data of the 2% sample (short dash line). (b) The difference of the Ni K-edge XAFS of the 2% sample with Ni edge data of NiO (long dash line), Ni acetate (dash-dot line), and the Cu edge data of the 2% sample (short dash line).

TABLE II. Environment about Cu(1), Cu(2), and average Cu in $YBa_2Cu_3O_{7-\delta}$

Atom	R (Å)	N Cu(1)	Cu(2)	Cu (average)
O	1.850	2	0	0.67
O	1.928	0	2	1.33
O	1.943	2	0	0.67
O	1.962	0	2	1.33
O	2.303	0	1	0.67
Y	3.205	0	4	2.67
Cu	3.373	0	1	0.67
Ba	3.381	0	4	2.67
Ba	3.473	8	0	2.67
O	3.659	0	4	2.67
Cu	3.823	2	2	2
Cu	3.886	2	2	2

indicating differences in the environment about the two atoms. The large nonlinear behavior indicates a large difference in the third moment of the near-neighbor oxygens. The calculated third moment about the Cu site is -7×10^{-5} Å^3 while the measured difference between the third moment about the Ni atoms and the Cu atoms is $+2 \times 10^{-3}$ Å^3. Thus, the third moment about the Ni atoms has a much larger magnitude than about the Cu atoms indicating a different site for the two.

The differences between the Ni and Cu sites are more obvious in the more distant shells. In Fig. 2 there is no obvious correspondence about the Cu site to the well-isolated second shell at 2.7 Å about the Ni. The shells beyond the first about the Cu atoms are composed of overlapping contributions from Y, Ba, Cu, and oxygen atoms (Table II). The k dependence of the second shell about the Ni indicates that it is not composed of oxygen atoms. The remaining possibilities are one or more of the four types of metallic atoms of Ni, Cu, Y, and Ba. To determine the atoms in the shell, comparisons were made with the

second shell of NiO for Ni backscatters and theoretical calculations[25] using spherical waves and a Dirac-Hara energy-dependent muffin-tin potential for the Ni center atom and the Cu, Y, and Ba backscattering atoms. The best fit, as shown in Fig. 4, occurred for $N=5.1\pm1.2$ Y backscatters at a distance of 2.96 ± 0.02 Å with $\sigma^2=0.011$ Å^2. A satisfactory fit also occurred for a mixture of Y atoms at 2.96 ± 0.02 Å and Ba atoms at 3.10 ± 0.02 Å but the relative number of Ba and Y atoms is not well determined. The rest of the shells beyond the second in the 2% Ni sample are too small to allow a reliable analysis.

The reliability of the theoretical fits can be assessed by comparing the measured spectra with the theory for the second shell Ni about the Ni center atom in NiO. Figure 5 shows such a fit. The variables in the fit are the distance R, σ^2, and the mean free path. The mean free path is defined by multiplying the theory by $S_0^2\exp[-2(R-\Delta)/\lambda]$ where $S_0^2=0.7$ is the factor introduced by the passive electrons,[23] and Δ is a correction due to the core of the center atom.[26] The values determined by the best fit are $\lambda=8$ Å, $R=2.94$ Å, and $\sigma^2=0.0046$ Å. The crystal structure value for R is 2.948 Å. As can be seen in Fig. 5, an excellent fit is obtained above $k=5$ Å^{-1}. The deviations above $k=9$ Å^{-1} are within the experimental errors. We are thus confident in our theoretical fits above $k=5$ Å^{-1}.

In comparing transmission experimental data with the theory, correction must be made for the fact that the experiment is normalized by the K-edge step while the theory is normalized by the K absorption at the energy. The correction was made using McMaster tables. For fluorescence data an additional correction must be made for the energy dependence of the absorption of x rays in the I_0 chamber. The assessment of a satisfactory fit was done using the standard[27] normalized goodness of fit criterion $\chi_\nu^2\lesssim1$. For Y, Ba, Ni, and Cu atoms in the second shell the respective values of χ_ν^2 are 0.26, 2.0, 6.1, and 29.

It is clear from these results that the Ni atoms do not simply substitute randomly, i.e., isomorphously for the Cu atoms, nor preferentially in one of the Cu sites. Table II lists the environment about the Cu(1) and the Cu(2) sites, separately. The presence of Y about the Ni in the second

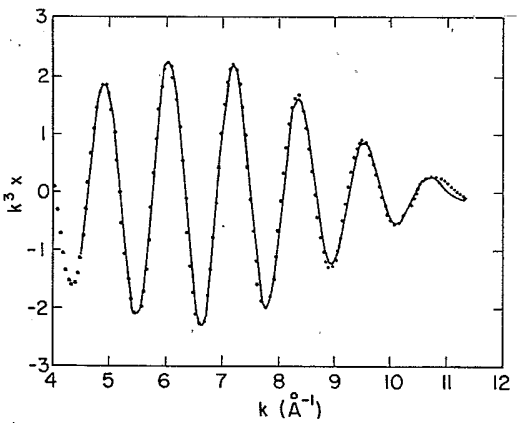

FIG. 4. The Y fit to the second shell data about the Ni impurities in the 2% Ni sample.

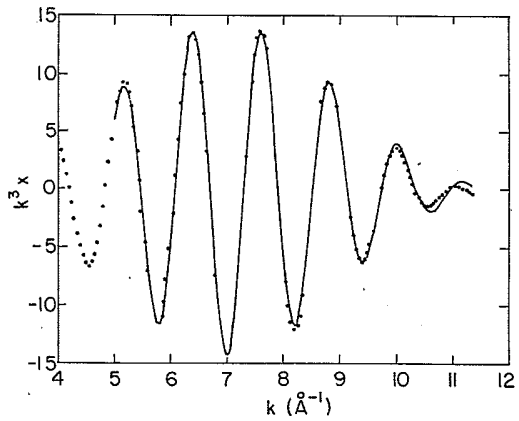

FIG. 5. The theoretical fit to the second shell Ni data in NiO.

shell is contrary to the substitution into the Cu(1) sites in the chains. Our results are also not consistent with preferential substitution on the Cu(2) planar sites since the Y and Ba distances are significantly in disagreement between the Ni atom and the Cu(2) site. It has been proposed that Ni substitutes on the Cu(2) planar sites based on one neutron-diffraction result,[13] though another neutron-diffraction analysis[28] found no evidence for the substitution of Ni on any Cu site. To make our results consistent with substitution on the Cu(2) planar sites requires an unphysical assumption, namely, that the Ni distorts the second and more distant neighbor environment much more than the first-neighbor environment. If the only perturbation is a substitution of Cu by Ni, the perturbation will decrease with distance from Ni. This is not the case indicating that the perturbation is not just localized at the Ni atom but occurs also in its surroundings, i.e., the surroundings also are changed and the Ni is not in a Cu site. This distortion not only decreases the distance to the Y atoms by 0.24 Å but also decreases the Ba atoms distances even more by 0.3 Å so that they overlap the Y atoms in the radial transform of Fig. 2. Such an overlap of Ba and Y atoms could be consistent with our result. However, such distortions can only occur by the Ni being in a different site than a Cu site.

NEAR-EDGE ANALYSIS

The final analysis we perform on the near-edge structure confirms that Ni does not substitute on any Cu site. Figure 6 shows near-edge scans of the Ni K edge for NiO, and the 2% Ni sample. Also shown is a corresponding Cu K edge for the 1:2:3 phase. These near-edge scans have the common features of the $3d$ "pip" denoted by A, and a rise to a main peak B. They are all aligned so that the onset of the $3d$ pip is in register in all cases. The environment about the Ni atoms in NiO has inversion symmetry. The $3d$ pip then has a contribution only from quadrupole transitions.[29] The energy difference between the $3d$ pip onset and the peak at B is also the same for NiO and the 2% Ni sample and for the Cu edge, indicating[30] that they all have the same valence of +2. The 2% Ni sample has, however, about twice the size of the $3d$ pip as the other Ni

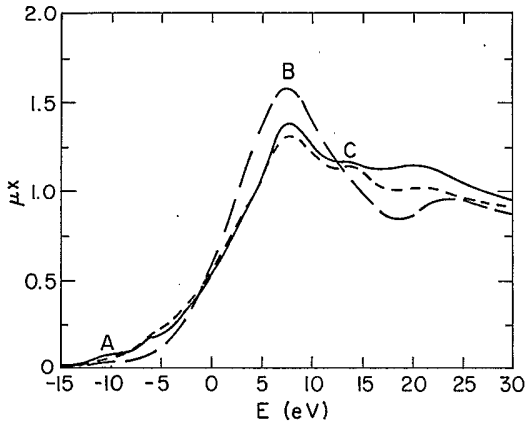

FIG. 6. Near-edge scans of the K edge of the Ni edges of the 2% sample (solid line), NiO (long dash line), and the Cu edge of the 2% sample (short dash line). The K-edge step has been normalized to one using the data beyond 30 eV. The onset of the $3d$ pip denoted by A has been aligned for all three edge scans. The features B and C are discussed in the text.

edge, indicating that it does not have an inversion symmetric environment, allowing a mixture of some p character and enhancing the transition with some dipole character. Comparing with the Cu edge, the transition is almost twice as large. Again, this is as expected if the asymmetry is almost the same as at the Cu site since Cu in the +2 state has about one half the number of d holes (one) as has Ni in the +2 state (two). This deviation from inversion symmetry for Cu occurs only in the planar Cu(2) site because of the puckering[24] of the oxygens out of the Cu plane.

The environment of the oxygens about the Ni in the 2% sample is more similar to that of the Cu than the NiO model as can be noted by comparing the rise of the absorption from the A to B features. However, there is a striking difference between the Ni and Cu near-K edge scans in the 1:2:3 sample in the feature marked C. That feature is significantly weaker in Ni than in Cu. The feature C has had an eventful history in the short period since x-ray absorption was applied to the high-T_c superconductors. Its existence had been argued as evidence of both +3 valence states[31] and of an antisite disorder[32] for the Cu atoms. However, from temperature and pressure dependence,[33,34] and more recently, from the polarization dependence,[35,36] it is clear that neither of the two interpretations is viable and feature C is a backscattering feature. Feature C has its largest magnitude when the x-ray polarization is parallel to the a-b plane and is weakened to the same extent as in the Ni K edge when the x-ray polarization is parallel to the c axis. This angular dependence contradicts both the interpretation of a +3 valence state and of antisite disorder. The Cu(1) site is the one that has been proposed to be in a +3 state. It would have about one-half the absorption for the a-b plane polarization than the c polarization since the Cu(1)-O plane is in the b-c plane. This is opposite to the actual measured polarization dependence. In the antisite disorder interpretation the feature C is caused by the Cu being in the Y site and sensing the Y−O bond distance. However, the expected polarization dependence at the Y site is small, again in contradiction to the measurement.

The polarization dependence of feature C indicates that the atoms producing it are mainly in the a-b plane of the Cu atoms. To ascertain which atoms cause the feature, we extended the background subtraction to lower energies so as to include the peak of feature C. For the analysis in the previous section the background did not include feature C. Although the background to include feature C is not well determined since it no longer is slowly varying relative to the XAFS signal, we are only interested in determining when feature C disappears, which is not sensitive to errors in the background subtraction.

The $k\chi(k)$ so obtained is shown in Fig. 7 by the dashed curve. The feature C peaks at $k=2$ Å^{-1}. The data are transformed into r space and windows are placed on the r-space data to isolate a region which is then back-transformed into k space. In Fig. 7 the back-transformed data from $0.4 \leq r \leq 6.08$ Å and from $6.08 \leq r \leq 11.6$ Å are shown. The feature C is present only in the latter range indicating that it is produced by a backscattering atom in that range. To minimize ringing introduced by the r-space window a Hanning function of full width 0.8 Å is placed at both ends of the window centered about the limits given above, which are at values where the Im part of the r-space transform passes through zero. Comparing the data from $6.08 \leq r \leq 11.6$ Å to the full $k\chi(k)$ data in Fig. 7 shows that negligible distortion is introduced by the window. Feature C begins to be significantly perturbed as the lower limit is extended to the range 6.9–11.6 Å and is reduced by a factor of 2 in the range 7.5–11.6 Å as shown in Fig. 7. Such an analysis indicates that the shell that produces feature C is centered somewhere between $6.9 < r < 7.5$ Å. To visualize more directly the region in r space that feature C contributes to, a transform starting at a lower k value of 1.5 Å^{-1} to include feature C and ending at $k=4.7$ Å^{-1} above which disorder smears out the contribution of interest, as shown in Fig. 7, is present-

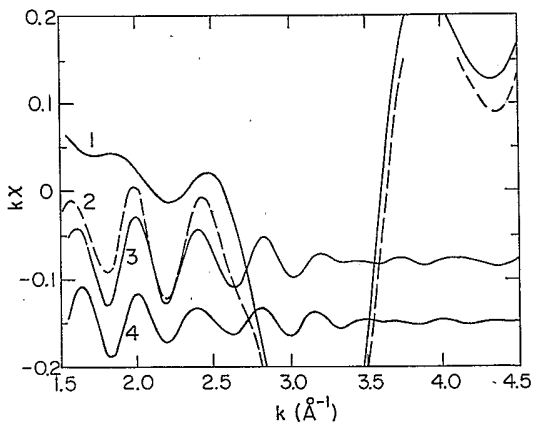

FIG. 7. Plots of $k\chi(k)$ showing the feature C of Fig. 6 at $k=2.0$ Å^{-1}. Curve 2 (dashed line) is the experimental data. Curve 1 is the data after a spatial filter $0.4 \leq r \leq 6.08$ Å. Curve 3 is after a spatial filter $6.08 \leq r \leq 11.6$ Å. Curve 4 is after a spatial filter $7.5 \leq r \leq 11.6$ Å.

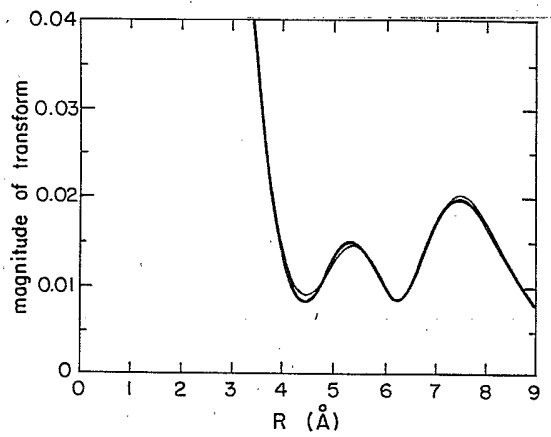

FIG. 8. The magnitude of transform of $k\chi(k)$ for $1.5 < k < 4.7$ Å^{-1} which emphasizes the contribution of atoms at large r. The thick line is an average over several scans while the thin line is a single scan. The difference between the two is a measure of the noise.

ed in Fig. 8. The thick solid curve in Fig. 8 is the average over several scans and the thin solid curve shows a typical single scan. The deviations are a measure of the noise in the data. As can be seen in Fig. 8, the peak in the region where feature C contributes is well defined, being much larger than the noise. Adding a shift of 0.4 Å introduced by the phase factor indicates that the shell of atoms that is producing feature C is in the range $7.3 < r < 7.9$ Å. The only metal atom in the Cu a-b plane at that range of distances[24] are Cu atoms which are two lattice constants ($2a$ or $2b - 7.7$ Å) away. The contribution of these atoms has a multiple scattering enhancement by the shadowing[23] of the intervening Cu atoms one lattice constant away.

The decrease of the strength of feature C about the Ni atoms indicates that at least most of them are not in either Cu site since each would produce a feature C, consistent with our previous analysis of the XAFS data. The advantage of the analysis of the feature C is its insensitivity to disorder because of its low value of $k = 2$ Å^{-1}. In order for disorder to reduce significantly this feature, the mean-square disorder $\sigma^2 = 1/2k^2 = 0.125$ Å.^{2} This corresponds to $\sigma = 0.35$ Å. It is quite unreasonable to expect such a large value of σ for the large distance of 7.7 Å from the perturbing Ni atom if it were at a Cu site, particularly when the first-neighbor oxygen atoms have a much smaller distortion.

SUMMARY AND CONCLUSION

We have found that Ni can dissolve into the 1:2:3 matrix up to a maximum of 4% of the Cu concentration, precipitating as NiO for higher concentration. The 1:2:3 matrix remains orthorhombic in structure but with a lowering of T_c down to 79.5 K for the highest concentration. The Ni atoms are in a valence state of +2. XAFS analysis shows that though the first-neighbor atomic environment about the Ni atoms remains somewhat similar to that about the Cu sites, the Ni does not substitute in either Cu site. This is shown both by the extended XAFS analysis and the near-edge XAFS analysis. The second shell of atoms around the Ni atoms is composed of either Y atoms at a distance of 2.96 ± 0.02 Å or a mixture of Y atoms at 2.96 ± 0.02 Å and Ba atoms at 3.10 ± 0.02 Å. This larger perturbation of distances at the second shell than at the first shell indicates that the perturbation is not localized at the Cu site but that the Ni atoms are in a different environment than the Cu atoms. The environment about the Ni atoms corresponds to no metallic site in the crystal structure. Because of noise in the data, it is not possible to exclude the possibility that a small fraction of the Ni atoms may be in Cu sites but our results are consistent with the statement that no substitution at Cu sites occurs.

We have determined where the Ni atoms are not located but it is not possible to determine where they are located. It is clear that they are not on any lattice site of the *perfect* crystal so, by the process of elimination, the Ni atoms are located on a defect site, either one already present in the pure 1:2:3 phase or one induced by the presence of the Ni impurities. It would take an analysis of the various defects in the material to hope to determine where the Ni is located, a project which is obviously very complicated and outside of the original intent.

The original intent to obtain more details about the electronic character of the Cu atoms and their environs which cause high T_c has been frustrated by the fact that Ni does not substitute on either Cu site, without a significant distortion of its environment. This feature is more evidence of the complicated nature of the 1:2:3 phase and the danger of thinking too naively about its properties. We had previously found[37] the pure 1:2:3 phase to be inhomogeneous. It was in a metastable state with significant microscopic structural variations of orthorhombicity $(b-a)/a$. Although Ni impurities do not substitute on the Cu sites, it would be unjustified to extrapolate this result to other impurities. At the same time, careful measurements should be made on other impurities to verify whether they do or do not substitute for the metal atoms that naively one would assume they do. In terms of the question of how Ni addition lowers T_c, our results show that the defect site occupied by the Ni atoms has that influence, presumably by destroying the perfection of the 1:2:3 phase. Such a perturbation is more drastic than a substitution for Cu and is consistent with the large effect of Ni alloying on T_c.

ACKNOWLEDGMENTS

The research of M. Qian, E. A. Stern, and Y. Ma was partially supported by the Division of Materials Science of the Department of Energy under Contract No. DE-AS05-80-ER10742. The research of Robert Ingalls was supported by the U.S. Department of Energy Grant No. DE-FG06-84ER45163. The research of M. Sarikaya, B. Thiel, R. Kurosky, C. Han, L. Hutter, and I. Aksay was sponsored by the Air Force Office of Scientific Research (AFOSR) and the Defense Advanced Research Projects

Agency (DARPA) under Grant No. AFOSR-87-0114. We thank B. Houser and J. E. Whitmore for their assistance. The x-ray spectra were taken at the Stanford Synchrotron Radiation Laboratory (SSRL) which is supported by the Department of Energy, the Office of Basic Energy Sciences and the National Institute of Health, the Biotechnology Resource Program, Division of Research Resources. We are indebted to the staff of SSRL for their invaluable help. The NiO XAFS data used in our analysis was graciously supplied by Ke Zhang.

[1]Y. Maeno, T. Tomita, M. Kyogoku, S. Awaji, Y. Aoki, K. Hoshino, A. Minami, and T. Fujita, Nature (London) **328**, 512 (1987).

[2]H. Hor, R. L. Meng, Y. Q. Wang, L. Gao, Z. J. Huang, J. Bechtold, K. Forster, and C. W. Chu, Phys. Rev. Lett. **58**, 1891 (1987).

[3]Y. Le Page, T. Siegrist, S. A. Sunshine, L. F. Schneemeyer, D. W. Murphy, S. M. Zahurak, J. V. Waszczak, W. R. McKinnon, J. M. Tarascon, G. W. Hull, and L. H. Greene, Phys. Rev. B **37**, 3617 (1987).

[4]X. D. Chen, F. Zuo, A. Chakraborty, B. R. Patton, J. R. Gaines, and A. J. Epstein, Bull. Am. Phys. Soc. **33**, 329 (1988).

[5]J. Jung, J. P. Franck, W. A. Miner, and M. A.-K. Mohamed, Bull. Am. Phys. Soc. **33**, 329 (1988).

[6]W. Murphy, S. A. Sunshine, R. B. van Dover, R. J. Cava, B. Batlogg, S. M. Zahurak, and L. F. Schneemeyer, Phys. Rev. Lett. **58**, 1888 (1987).

[7]J. Bechtold, P. H. Hor, R. L. Meng, L. Gao, Z. J. Huang, Y. Y. Sun, Y. Q. Wang, and C. W. Chu, Bull. Am. Phys. Soc. **33**, 329 (1988).

[8]S. A. Shaheen, G. Ling, F. Lu, Y. Jeon, M. Croft, N. Jisrawi, and W. L. McLean, Bull. Am. Phys. Soc. **33**, 329 (1988).

[9]I. Felner, I. Nowik, and Y. Yeshurun, Phys. Rev. B **36**, 3923 (1987).

[10]Y. Maeno, T. Nojima, Y. Aoki, M. Kato, K. Hoshino, A. Minami, and T. Fujita, Jpn. J. Appl. Phys. **26**, L774 (1987).

[11]J. W. Tarascon, L. H. Greene, P. Barboux, W. R. McKinnon, G. W. Hul, T. P. Orlando, K. A. Delin, S. Foner, and E. J. McNiff, Jr., Phys. Rev. B **35**, 8393 (1987).

[12]Gang Xiao, F. H. Streitz, A. Gavrin, Y. W. Du, and C. L. Chien, Phys. Rev. B **35**, 8782 (1987).

[13]L. H. Greene, Bull. Am. Phys. Soc. **33**, 212 (1988).

[14]S. N. Song, J. Thiel, K. R. Poeppelmeier, and J. B. Ketterson, Bull. Am. Phys. Soc. **33**, 329 (1988).

[15]C. L. Chen, Bull. Am. Phys. Soc. **33**, 346 (1988).

[16]K. Elgaid, C. Blue, I. Zitkovsky, W. Hiff, D. McDanier, and P. Boolchand, Bull. Am. Phys. Soc. **33**, 560 (1988).

[17]K. Zhang, G. Bunker, B. Chance, and R. C. Yu (unpublished).

[18]F. Bridges, J. B. Boyce, T. Claeson, R. S. Howland, T. H. Geballe, and J. M. Tarascon, Bull. Am. Phys. Soc. **33**, 560 (1988).

[19]N. J. Zalurec, in *Introduction to Analytical Electron Microscopy,* edited by J. J. Hren, J. I. Goldstein, and D. C. Joy (Plenum, New York, 1979), p. 121.

[20]M. Sarikaya and B. Thiel, J. Am. Ceram. Soc. **71**, 9373 (1988).

[21]E. E. Underwood, *Quantitative Stereology* (Addison-Wesley, New York, 1970).

[22]E. A. Stern and S. M. Heald, Rev. Sci. Instrum. **50**, 1579 (1979).

[23]E. A. Stern and S. M. Heald, in *Handbook on Synchrotron Radiation,* edited by E. E. Koch (North-Holland, New York, 1983), Vol. 1, p. 955.

[24]M. A. Beno, L. Soderholm, D. W. Capone II, D. G. Hinks, J. D. Jorgensen, Ivan K. Schuller, C. U. Segre, K. Zhang, and J. D. Grace, Appl. Phys. Lett. **51**, 57 (1987).

[25]J. J. Rehr and J. Muestre (private communication).

[26]E. A. Stern, B. A. Bunker, and S. M. Heald, Phys. Rev. B **21**, 5521 (1980).

[27]P. R. Bevington, *Data Reduction and Error Analysis for the Physical Sciences* (McGraw-Hill, New York, 1969).

[28]J. J. Ryne (private communication).

[29]R. A. Bair and W. A. Goddard III, Phys. Rev. B **22**, 2767 (1980).

[30]G. Bunker, E. A. Stern, R. E. Blankenship, and W. W. Parson, Biophys. J. **37**, 539 (1982).

[31]E. E. Alp, G. K. Shenoy, D. G. Hinks, D. W. Capone II, L. Soderholm, H.-B. Schuttler, J. Guo, D. E. Ellis, P. A. Montano, and M. Ramanthan, Phys. Rev. B **35**, 7199 (1987).

[32]F. W. Lytle, R. B. Greegor, and A. J. Panson, Phys. Rev. B **37**, 1550 (1988).

[33]J. M. Tranquada, S. M. Heald, A. R. Moodenbaugh, and M. Suenaga, Phys. Rev. B **35**, 7187 (1987).

[34]E. D. Crozier, N. Alberding, K. R. Bauchspiess, A. J. Seary, and S. Gygaux, Phys. Rev. B **36**, 8288 (1987).

[35]S. M. Heald, J. M. Tranquada, A. R. Moodenbaugh, and Youwen Xu, Phys. Rev. B **38**, 761 (1988).

[36]J. Whitmore, M. Qian, E. A. Stern, R. Ingalls, and Y. Ma (unpublished).

[37]M. Sarikaya and E. A. Stern, Phys. Rev. B **37**, 9373 (1988).